Spin-wave resonances in $La_{0.7}Sr_{0.3}MnO_3$ films: Measurement of spin-wave stiffness and anisotropy field

M. Golosovsky* and P. Monod
Laboratoire de Physique du Solide, ESPCI, 10 rue Vauquelin, 75231 Paris Cedex 05, France

P. K. Muduli and R. C. Budhani
Department of Physics, Indian Institute of Technology, Kanpur, 208016, India

(Received 18 June 2007; revised manuscript received 23 September 2007; published 13 November 2007)

We studied magnetic-field-dependent microwave absorption in epitaxial $La_{0.7}Sr_{0.3}MnO_3$ films using an 9.5 GHz Bruker electron-spin-resonance spectrometer. By analyzing the angular and temperature dependence of the ferromagnetic and spin-wave resonances we determine spin-wave stiffness and perpendicular anisotropy field. The spin-wave stiffness as found from the spectrum of the standing spin-wave resonances in thin films is in fair agreement with the results of inelastic neutron scattering studies on a single crystal of the same composition [L. Vasiliu-Doloc *et al.*, J. Appl. Phys. **83**, 7343 (1998)].

DOI: 10.1103/PhysRevB.76.184413 PACS number(s): 76.50.+g, 75.30.Ds, 75.40.Gb

I. INTRODUCTION

Spin-wave stiffness D is an important parameter of magnetic materials that characterizes the magnon dispersion law $\omega = Dk^2$. In the mean-field approximation it is directly related to the exchange integral J—namely,

$$D = \frac{2JSa^2}{\hbar}, \tag{1}$$

where a is the lattice constant and S is the spin.[1] Inelastic neutron scattering studies of the spin-wave stiffness in manganite single crystals[2–7] revealed important information on the nature of their ferromagnetic transition. Since this issue is under debate,[7,8] it is important to study spin-wave stiffness more closely—in particular, to measure D in thin films. It is also important to explore complementary techniques. In principle, spin-wave excitations can be measured using the magneto-optical Kerr effect or Brillouin light scattering,[9] although existing studies of manganites by these methods[10,11] do not focus on spin waves.

Spin-wave stiffness has been traditionally measured by the microwave absorption technique: using a fixed frequency electron-spin-resonance (ESR) spectrometer[9,12] or broadband techniques.[13] Several groups reported fixed-frequency microwave studies of standing spin-wave resonances (SWRs) in $La_{0.67}Ba_{0.33}MnO_3$ (Ref. 14) and $La_{0.7}Mn_{1.3}O_3$ (Refs. 15–17) thin films. Although spin-wave excitation at microwave frequencies was observed in $La_{0.75}Sr_{0.11}Ca_{0.14}MnO_3$ (Ref. 18), $La_{0.7}Ca_{0.3}MnO_3$ (Ref. 19), and $La_{0.7}Sr_{0.3}MnO_3$ (Ref. 20) thin films, it was not studied in detail.

In contrast to inelastic neutron scattering that (i) measures traveling spin waves with large wave vectors $k \sim 1-0.1$ Å^{-1} and (ii) requires large single crystals; the microwave absorption technique measures the spectrum of standing spin-wave resonances with small wave vectors $k \sim 10^{-2}-10^{-3}$ Å^{-1} and operates mostly with thin films. The recent overview of spin-wave excitations in manganites[21] compares thin-film microwave absorption measurements to inelastic neutron scattering studies of single crystals. It turns out that there is no manganite compound that was studied simultaneously by both techniques. Our present work fills this gap. We study the spin-wave spectrum in epitaxial $La_{0.7}Sr_{0.3}MnO_3$ films of different thicknesses and on different substrates by the microwave absorption technique at 9.4 GHz and compare our data to inelastic neutron scattering studies on single crystals of the same composition.

II. STANDING SPIN-WAVE RESONANCES IN A THIN FERROMAGNETIC FILM

Consider a thin ferromagnetic film with an "easy-plane" magnetic anisotropy. The magnetic field is oriented at an oblique angle Ψ with respect to the film normal. The orientation of magnetization, Θ, is determined by the interplay between the external field H and the perpendicular anisotropy field H_a and is found from the equation[12,22]

$$H_a \sin\Theta \cos\Theta = H \sin(\Theta - \Psi), \tag{2}$$

where in-plane anisotropy has been neglected. In the presence of a microwave magnetic field with frequency ω, whereas $h_{mw} \perp H$, the SWRs are excited. The resonance field H is found from the condition[12,22]

$$\omega^2 = [\gamma H \cos(\Theta - \Psi) - \gamma H_a \cos^2\Theta + Dk^2] \times [\gamma H \cos(\Theta - \Psi) - \gamma H_a \cos 2\Theta + Dk^2] \tag{3}$$

where γ is the gyromagnetic ratio. If surface spins are completely pinned or completely unpinned, then

$$k = \pi n/d, \tag{4}$$

where d is the film thickness and n is an integer. The uniform ferromagnetic resonance (FMR) mode corresponds to $n=0$, while the spin-wave resonances correspond to $n \neq 0$. For the perpendicular orientation ($\Psi = \Theta = 0$), Eq. (3) yields

$$H_n - H_0 = H_a - \frac{\pi^2 n^2}{\gamma d^2} D, \tag{5}$$

where $H_0 = \frac{\omega}{\gamma}$ and ω is the microwave frequency. To determine D, one measures microwave absorption in dependence

of the magnetic field and notices a sequence of resonances. By analyzing their spectrum using Eq. (5) one identifies mode numbers n. The slope of the linear dependence, H_n vs n^2, yields D, while the intercept with the H axis yields H_a. To enable such a procedure the film thickness should lie in certain limits

$$\delta \gg d \gg \pi \left[\frac{D}{\gamma(H_0 + H_a)} \right]^{1/2}, \tag{6}$$

where δ is the skin depth. Indeed, for efficient excitation of the spin-wave resonances the film thickness should be smaller than the skin depth. On the other hand, the film should be thick enough to support several resonances.

III. EXPERIMENT

Our experiments were performed with a bipolar X-band Bruker ESR spectrometer, a TE_{102} resonant cavity, and an Oxford cryostat. We studied $La_{0.7}Sr_{0.3}MnO_3$ films (d=50, 100, 150, and 200 nm) grown on a (001) $SrTiO_3$ substrate (STO) and $La_{0.67}Sr_{0.33}MnO_3$ films (d=50 and 150 nm) on a $NdGaO_3$ substrate (NGO). The samples were fabricated by pulsed laser deposition[24] and were cut to small millimeter-size pieces in order to keep a reasonable value of the cavity Q factor. We measured magnetization and resistivity of these films by superconducting quantum interference device (SQUID) magnetometry and four-point technique, correspondingly. The skin depth at 9.4 GHz estimated from our resistivity measurements[23]—22 μm at 295 K and 5 μm at 50 K—considerably exceeds the film thickness.

The film uniformity could be estimated from the FMR spectrum. A uniform film is characterized by a narrow FMR peak, corresponding to a well-defined anisotropy field, while a nonuniform film usually exhibits a broad FMR peak, indicating a wide spread of the anisotropy fields. Most of our samples demonstrated a narrow FMR peak at ambient temperature, although some samples showed several narrow FMR peaks corresponding to discrete values of the anisotropy field.

IV. EXPERIMENTAL RESULTS

A. $La_{0.7}Sr_{0.3}MnO_3$ films on the $SrTiO_3$ substrate

Figure 1 shows microwave absorption derivative in the perpendicular field for a 200-nm-thick $La_{0.7}Sr_{0.3}MnO_3$ film on the $SrTiO_3$ substrate. We observe a series of slightly asymmetric narrow peaks. The asymmetry changes slowly with temperature and is attributed to the coupling to the dielectric resonances in the STO substrate and was observed in other studies as well.[20,23] The angular dependence of the resonant fields (not shown here) follows Eq. (5); hence, we attribute these peaks to the spin-wave resonances. We cut the original 5×5 mm^2 film to five pieces with the size of 1×0.5 mm^2, and all these pieces demonstrated fairly identical spectra. The very fact that we observe sharp and reproducible resonances proves that the film is highly uniform. Another indication of the high quality of the film is the narrow peak-to-peak linewidth (16 Oe at ambient temperature) and low coercive field (11–16 Oe at 295 K).

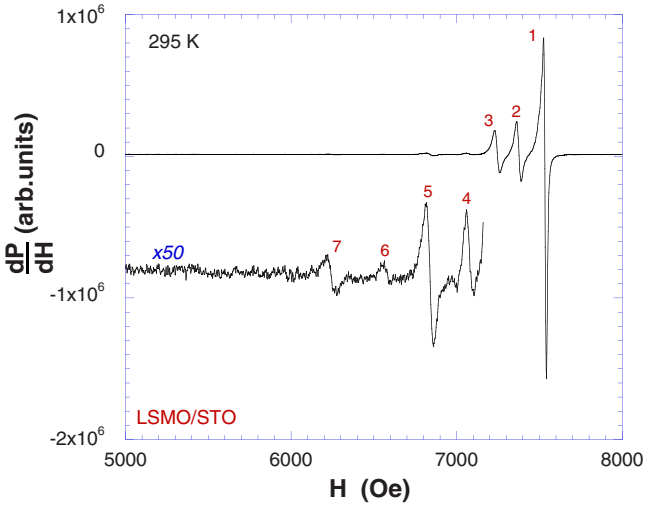

FIG. 1. (Color online) Absorption derivative spectrum for a 200-nm-thick $La_{0.7}Sr_{0.3}MnO_3$ film on the $SrTiO_3$ substrate in the perpendicular magnetic field. The mode number is shown at each peak. The microwave frequency is 9.4 GHz, the incident power is P_{mw}=0.2 mW (−30 dB), and the modulation field is 10 Oe.

The mode numbers were established as follows. We assigned consecutive numbers to the peaks in Fig. 1 and checked whether the linear dependence $H_n \propto n^2$, predicted by Eq. (5), holds. The best correspondence to Eq. (3) was achieved for the sequence $n=1,2,3,\ldots$ or $n=0,2,3,\ldots$. There is some ambiguity in whether the strongest peak corresponds to $n=0$, to $n=1$, or to their sum, since the splitting between the $n=0$ and the $n=1$ modes as predicted by Eq. (5) is only 25 Oe and this is comparable to the linewidth.

Figure 2 shows SWR intensities and linewidths. The linewidth increases almost linearly with mode number, while the intensity decreases. Odd modes have generally higher intensities than even modes (see also Fig. 1).

Figure 3 shows the dependence of the resonance fields on the mode number. The higher-order modes obey a quadratic dependence, $H_n \propto n^2$, while the modes with low n show a tendency to linear spacing that is quite common for films with surface pinning.[25] We exclude from our analysis the first two modes that should be most strongly affected by surface pinning and determine spin-wave stiffness from the slope of H_n vs n^2 dependences using Eq. (5). The results are shown in Fig. 4.

To find the perpendicular anisotropy field we extrapolate the H_n vs n^2 dependences to n=0. Equation (7) and Fig. 3 yield H_a=0.4 T at 295 K and H_a=1 T at 4.2 K. To analyze these values we note that the perpendicular anisotropy field of a thin film,

$$H_a = H_{demag} + H_{cryst} + H_{stress}, \tag{7}$$

consists of a demagnetizing field $4\pi M$, crystalline anisotropy H_{cryst}, and stress-induced anisotropy H_{stress}. The crystalline anisotropy of $La_{0.7}Sr_{0.3}MnO_3$ is very small[26,27] and does not exceed 0.03 T.[28] The demagnetization field as esti-

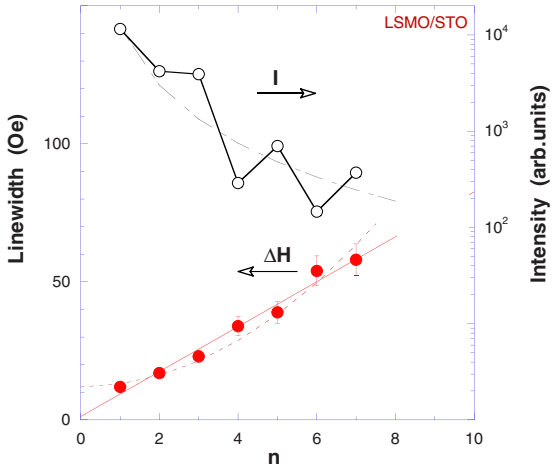

FIG. 2. (Color online) The solid symbols indicate the SWR linewidth ΔH_n, the red solid line shows linear fit [Eq. (9)], and the red dashed line shows quadratic fit [Eq. (8)]. The open symbols indicate the integrated SWR intensity corrected for the linewidth, $I=I_{pp}(\Delta H)^2$. Here, I_{pp} is the peak-to-peak magnitude of the absorption derivative. The black solid line here is a guide to the eye, the dashed black line shows Kittel's $1/n^2$ prediction (Ref. 1). The sample is a 200-nm-thick $La_{0.7}Sr_{0.3}MnO_3$ film on the $SrTiO_3$ substrate at ambient temperature.

mated from magnetization[26,27] is $H_{demag}=0.74$ T at 4.2 K. Since the lattice mismatch between $La_{0.7}Sr_{0.3}MnO_3$ and $SrTiO_3$ is only 1.4% and the film is sufficiently thick, the H_{stress} is not high and achieves considerable magnitude only at low temperatures.[29] Equation (7) yields the stress anisotropy field $H_{stress}=0.26$ T at 4.2 K. This means that even

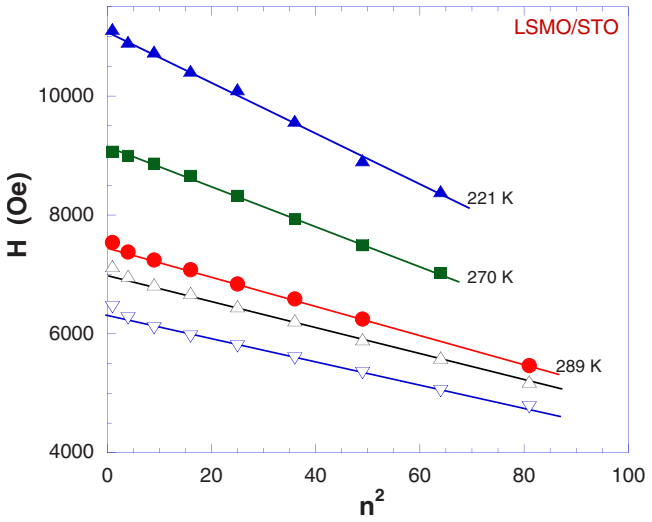

FIG. 3. (Color online) The resonance field of different modes for the film shown in Fig. 1. Solid symbols indicate the data measured at fixed and known temperatures and at low microwave power $P_{mw}=0.2$ mW. Open symbols indicate the data measured at ambient temperature and increased microwave power (62.5 mW and 200 mW, correspondingly). Here, the sample temperature is higher than the ambient temperature due to self-heating. The lines show the $H_n \propto n^2$ approximation.

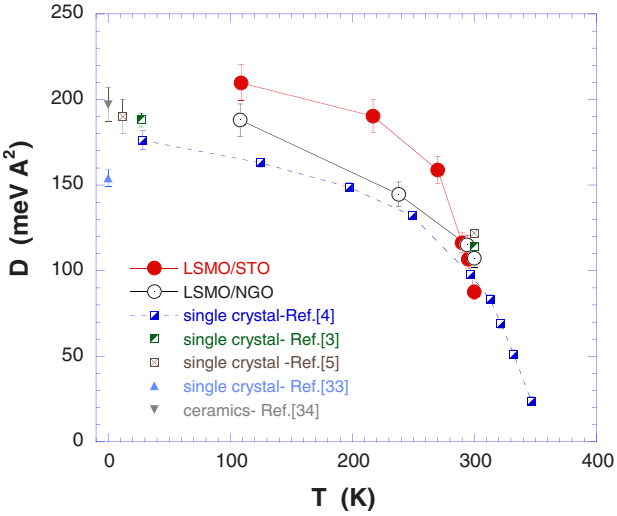

FIG. 4. (Color online) Temperature dependence of the spin-wave stiffness $D(T)$. The circles stand for our microwave measurements on thin films on substrate. The squares show inelastic neutron scattering data for the $La_{0.7}Sr_{0.3}MnO_3$ single crystals. The triangles stand for the $D^{Bloch}(T=0)$ estimated from the temperature dependence of magnetization and $T^{3/2}$ Bloch law. The lines are a guide to the eye.

at low temperatures the demagnetization field is the dominant contribution to the anisotropy field. This is consistent with other measurements. Indeed, magnetization studies of Ref. 27 for films of comparable thickness found that $H_{demag}=0.8H_a$ at 10 K, while Ref. 26 found that $H_{demag}=0.95H_a$ at 295 K.

B. $La_{0.67}Sr_{0.33}MnO_3$ films on the $NdGaO_3$ substrate

Figure 5 shows the microwave absorption spectrum for a 150-nm-thick $La_{0.67}Sr_{0.33}MnO_3$ film on the $NdGaO_3$ substrate at 108 K. We observe a strong and narrow peak at 10445 Oe and a series of low-field satellites. The peak-to-peak linewidth of the dominant resonance is very small (12 Oe at ambient temperature and 33 Oe at 108 K), and this proves the high quality of the film. The coercive field at ambient temperature is only 4 Oe. We cut the film to several pieces and they showed consistent spectra.

To identify the resonances we measured temperature and angular dependences of the resonant field and came to the conclusion that the peaks designated with integer numbers in Fig. 5 are spin-wave satellites of the peak at 10 445 Oe, while the strong peak at $H=7470$ Oe does not belong to this series. Indeed, the angular dependences of the resonant field of the numbered peaks are very similar (not shown here) and different from that for the peak at 7470 Oe. The same is true with respect to the temperature dependences. We attribute the peak at 7470 Oe to the region with a different discrete value of the anisotropy field and exclude it from the subsequent analysis.

Figure 6 shows that the resonant fields of higher modes follow $H_n \propto n^2$ dependence. The slope of this dependence (the first mode excluded) yields the spin-wave stiffness D. The results are plotted in Fig. 4. The same data yield the

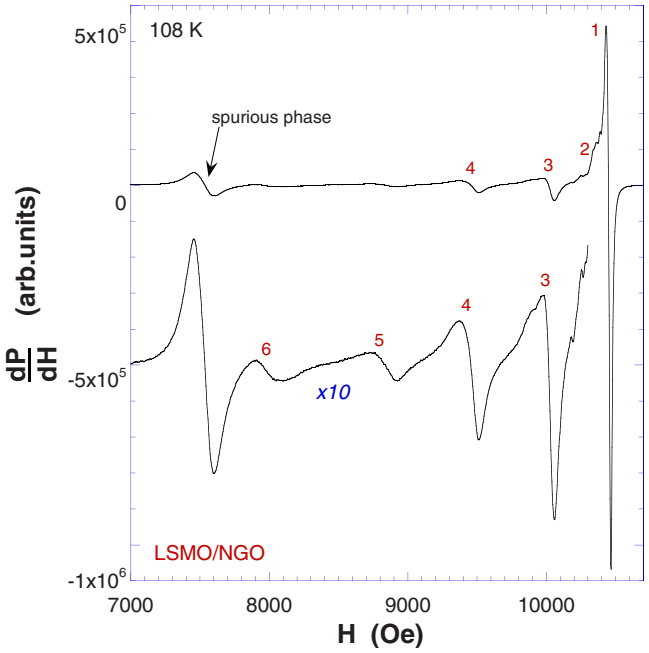

FIG. 5. (Color online) Absorption derivative spectrum for a 150-nm-thick $La_{0.67}Sr_{0.33}MnO_3$ film on the $NdGaO_3$ substrate. The mode number is shown at each peak. A strong peak at $H=7470$ Oe originates from the ferromagnetic resonance in a region of the film with the different anisotropy field.

perpendicular anisotropy field. We find $H_a=0.73$ T at 4.2 K. This is almost equal to the demagnetizing field, $4\pi M=0.74$ T, and means that the stress-induced anisotropy is negligible here, as expected for the lattice-matched substrate. The linewidth (see inset) steadily increases with n.

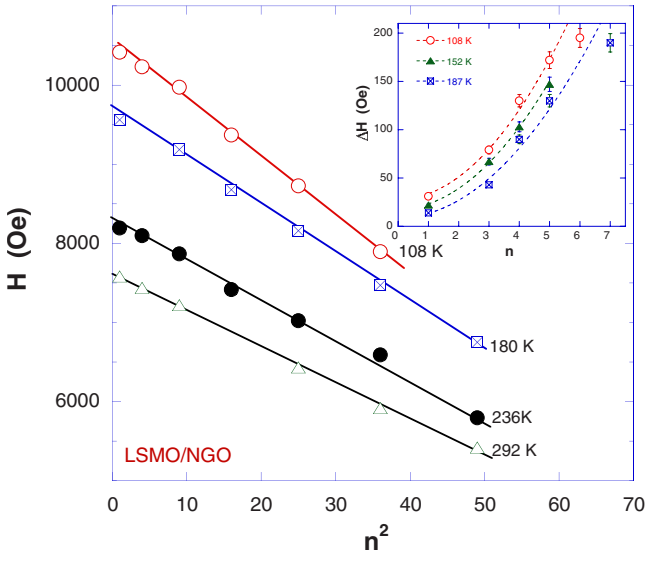

FIG. 6. (Color online) Resonance field of the SWR modes at several temperatures for the sample shown in Fig. 5. The lines show $H_n \propto n^2$ approximation. The inset shows linewidth vs mode number. The dashed lines in the inset show quadratic approximation [Eq. (8)].

C. Other films

We observed spin-wave resonances in several films with different thickness. In a very thin ($d=50$ nm) $La_{0.67}Sr_{0.33}MnO_3$ film on $SrTiO_3$ we observed only one spin-wave resonance which was displaced down by 0.23 T from the dominant FMR resonance [while Eq. (5) predicts 0.08 T]. Such a pronounced displacement is obviously related to strong surface pinning; hence, it is not possible to measure D there. In several 150-nm-thick $La_{0.67}Sr_{0.33}MnO_3$ films on $SrTiO_3$ we observed two overlapping series of spin-wave resonances, so that determination of D here was ambiguous. Reference 17 observed such split spin-wave resonances in a 350-nm-thick $La_{0.7}Mn_{1.3}O_3$ film on $LaAlO_3$ substrate and showed that the splitting disappears after annealing in oxygen. Following Ref. 17 we studied the effect of oxygen annealing on the SWR spectra in our films. Contrary to Ref. 17 we found that oxygen annealing at different temperatures from 600 °C to 900 °C does not ameliorate the SWR spectrum in our films but introduces additional splitting. In particular, the resonant peaks in annealed films split into many narrow lines with a spacing of ~15 Oe. The difference between our results and those of Ref. 17 is probably related to the fact that we operate with a film of different composition and on a different substrate.

V. DISCUSSION

A. Zero-temperature spin-wave stiffness

Figure 4 compares the spin-wave stiffness found in our microwave absorption studies of $La_{0.7}Sr_{0.3}Mn_{0.7}O_3$ thin films to inelastic neutron scattering measurements on single crystals of the same composition.[3–5] Consider first the limit $T=0$. Our measurements for two films of different thickness yield $D_0^{film}=210$ meV Å^2 while the corresponding neutron scattering data show lower values, $D_0^{cryst}=188$ (Ref. 3), 170 (Ref. 2), 176 (Ref. 4), and 190 (Ref. 5) meV Å^2. It is unlikely that the discrepancy between D_0^{film} and D_0^{cryst} arises from the fact that few atomic layers adjacent to the film-substrate interface could be nonmagnetic. In LSMO this "dead layer" may be up to 5 nm thick,[30,31] and hence "magnetic" thickness that appears in Eq. (5) can be smaller than the nominal thickness. The correction for the dead layer can bring down D_0^{film} by 5%.

The spin-wave stiffness at $T=0$ can be also estimated from the temperature dependence of magnetization and the $T^{3/2}$ Bloch law (see also Ref. 32). For the $La_{0.7}Sr_{0.3}MnO_3$ single crystals this yields $D_0^{Bloch}=154$ meV Å^2 (Ref. 33), while for ceramics of the same composition, $D_0^{Bloch}=197$ meV Å^2 (Ref. 34).

B. Temperature dependence

Consider now the temperature dependence of the spin-wave stiffness. Figure 4 shows that the results for two films with different thicknesses and on different substrates (one with tensile stress and another with a weak compressive stress) are very close, as expected for intrinsic properties. At ambient temperature, we find for these two films $D^{film}=104$ and 114 meV Å^2, correspondingly. This is almost identical to

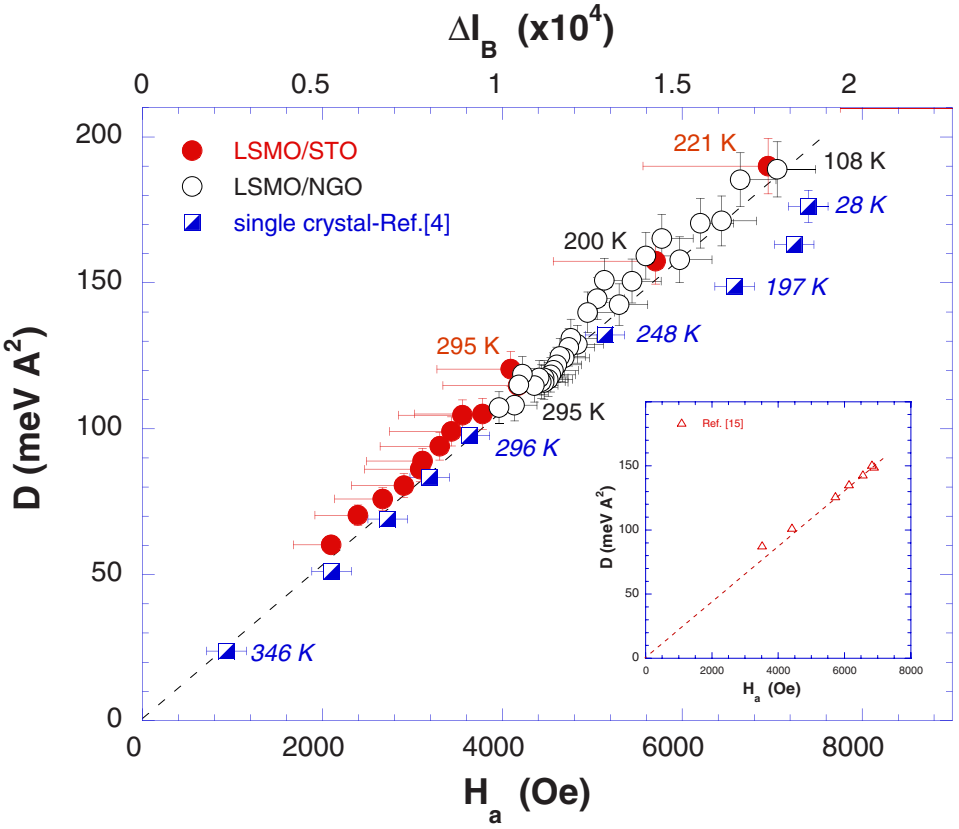

FIG. 7. (Color online) Spin-wave stiffness versus magnetization at varying temperature. The circles stand for our microwave measurements on thin films. As a measure of magnetization we take the perpendicular anisotropy field H_a (lower horizontal scale). The squares stand for the single-crystal data measured by the inelastic neutron scattering technique (Ref. 4). As a measure of magnetization in this case we take the integrated intensity of the electronic Bragg peak (upper horizontal scale). The dashed line shows the linear approximation. The inset shows a similar $D(M)$ dependence for the $La_{0.7}Mn_{1.3}O_3$ film as extracted from the microwave absorption measurements of Refs. 15 and 16.

the single-crystal data at ambient temperature: $D^{cryst}=114$ (Ref. 3) and 100 meV Å^2 (Ref. 4). However, one should take into account the difference in T_C as well.

C. Comparison between the samples

In order to compare data for the samples with different T_C we consider $D(T)$ vs $M(T)$ plots where the temperature is an implicit variable. A similar plot was used earlier by Ref. 35 to compare spin-wave stiffness of the Fe-Cr alloys with different composition and different T_C. The rationale behind such plot is the mean-field expression—Eq. (1)—which in fact relates the spin-wave stiffness to magnetization, $M=g\mu_B S/V_a$. Here, μ_B is the Bohr magneton, g is the g factor, and $V_a \propto a^3$ is the atomic volume. Equation (1) yields direct proportionality, $D \propto JM$. Strictly speaking, this proportionality is expected only for the Heisenberg model and at $T=0$. However, since M and D both go to zero at T_C, then we expect that the $D \propto M$ proportionality holds up to T_C. Indeed, as Ref. 36 shows, empirical data for many ferromagnetic compounds suggest that D and M have the same temperature dependence in the whole range from $T=0$ to $T=T_C$.

To effectuate this approach we plot D vs M (Fig. 7) where D and M are measured at the same temperature.[37] We find D from the microwave absorption spectra, while the magnetization is estimated indirectly from the anisotropy field H_a. Indeed, since the dominant contribution to H_a in our films is the demagnetizing field $4\pi M$ (especially for the films on NGO), hence the perpendicular anisotropy field is a measure of magnetization.

Figure 7 plots the spin-wave stiffness versus anisotropy field where the temperature is an implicit parameter. It also plots the corresponding single crystal neutron-scattering data of Ref. 4 where magnetization was estimated from the intensity of the electronic Bragg peak. The upper horizontal scale in Fig. 7 was chosen in such a way that the low-temperature limit of the electronic Bragg peak intensity ($\Delta I_B=1.85\times10^4$) corresponds to the saturation magnetization of $La_{0.7}Sr_{0.3}MnO_3$—i.e., $4\pi M=0.74$ T. The horizontal error bars in our thin-film measurements take into account the possible difference between the anisotropy field and magnetization arising from the stress anisotropy field [Eq. (7)]. We assume extreme values of $H_{stress}/4\pi M=-0.06$ and 0.2 for the films on NGO and STO, correspondingly.

We observe that above $T=295$ K the data for both our films and for the single crystal collapse. The resulting $D(M)$ dependence is quasilinear, which indicates the same critical indices of D and M at T_C. This is not obvious since the neutron scattering measurements were performed in zero magnetic field while the microwave measurements were performed in a finite field of 0.4–1 T. Using Eq. (1) we find the same value of the exchange integral, $J=3.6$ meV (for $S=1.85$ and $a=3.88$ Å) for the film and single crystal. This is also not obvious since thin films are strained.

We processed in the same way the microwave absorption data of Refs. 15 and 16 for the film of different composition: $La_{0.7}Mn_{1.3}O_3$ (see inset in Fig. 7). While $D(M)$ proportionality holds at low temperatures, there is an upward deviation as $T \to T_C$. This suggests a discontinuous variation of D across the ferromagnetic transition. Our data for the $La_{0.7}Sr_{0.3}MnO_3$ films do not indicate such a discontinuity.

D. Linewidth

The linewidth that steadily increases with mode number (Figs. 2 and 6) is not frequently observed in microwave absorption studies of spin-wave resonances. Previous studies of Permalloy films and other highly conducting ferromagnets found a weak and nonmonotonous dependence $\Delta H(n)$. (Refs. 38–42) Such a nonmonotonous dependence arises from the sum of several sources such as eddy-current damping, surface roughness, and fluctuations (exchange energy, anisotropy field, thickness).[43]

The k-dependent linewidth observed in our studies could be hardly intrinsic. Indeed, the theoretical prediction for the magnon-magnon scattering in manganites yields an inverse spin lifetime $\Gamma \propto k^4$ (Ref. 44). The neutron scattering studies of $La_{0.85}Sr_{0.15}MnO_3$ single crystals[6] indeed yield $\Gamma = 3050k^4$ (here k is in $Å^{-1}$ and Γ is in meV). Extrapolation of this k^4 dependence (obtained for 10 K and $k=0.02-0.16$ $Å^{-1}$) down to the range of wave vectors occurring in our microwave studies ($k_{max}=0.014$ $Å^{-1}$) yields $\Gamma = 1.1 \times 10^{-4}$. This is much smaller than what we observe in Fig. 2: $\Gamma = \Delta H/\gamma = 4.7 \times 10^{-3}$ (note, however, that our films have different composition as compared to those studied in Ref. 6). This indicates that the k-dependent linewidth found in our studies in thin films is extrinsic. It most probably arises either from the inhomogeneous broadening associated with thickness nonuniformity[41] or from the spin-wave scattering on the surface and bulk disorder.[45–47]

If we take an extreme approach and assume only thickness nonuniformity, then Ref. 41 yields

$$\Delta H_d = \Delta H_0 + \frac{2D\pi^2 n^2}{d^3}\Delta d, \tag{8}$$

where ΔH_0 is the linewidth of the uniform precession mode and Δd is the average thickness variation. Analysis of our data according to Eq. (8) (dashed lines in Figs. 2 and 6) yields $\Delta d = 4$ nm (2%) and 6 nm (4%) for the films on STO and NGO, correspondingly.

If we go to another extreme and assume spin-wave scattering to be the only source of line broadening, then according to the transit-time treatment[47] we find

$$\Delta H_{sc} - \Delta H_0 = \frac{v_g}{\gamma l_{sc}} = \frac{2D\pi n}{\gamma d l_{sw}}, \tag{9}$$

where $v_g = 2Dk$ is the group velocity and l_{sw} is the mean free path. Spin-wave scattering on bulk disorder is characterized by the combination of linear and quadratic k dependences,[45,46] whereas the linear k dependence implies a constant mean free path. Analysis of our data according to Eq. (9) and assuming constant l_{sw} yields $l_{sw}/d = 2$ for the LSMO/STO film at ambient temperature (Fig. 2). For the LSMO/NGO film (Fig. 6) we find $l_{sw}/d = 1.4$ and 1.3 at 108 K and at 187 K, correspondingly. The spin-wave mean free path being on the order of the film thickness suggests that the scattering occurs predominantly at film interfaces. Such scattering may result from surface roughness[48] or from the localized Mn^{4+} ions[31] or Mn^{2+} ions[49] at the film surface.

The observed k dependence of the linewidth is most probably due to both mechanisms: thickness nonuniformity and scattering. Note, however, that both extreme approaches [Eqs. (8) and (9)] yield a long mean free path that practically excludes bulk scattering. This is surprising, since the stoichiometry of $La_{0.7}Sr_{0.3}MnO_3$ suggests two possible states of Mn ion: Mn^{3+} with spin $S=3/2$ and Mn^{4+} with spin $S=2$. If $La_{0.7}Sr_{0.3}MnO_3$ were a Heisenberg ferromagnet, this would certainly result in magnetic inhomogeneity. However, observation of standing spin-wave resonances with high mode numbers indicates negligible bulk scattering and a single magnetic state of Mn ions in the bulk, as was already established by NMR studies of ^{55}Mn in $La_{0.67}Sr_{0.33}MnO_3$ (Ref. 31).

E. Other manganite compounds

The standing spin-wave resonances have been observed so far in the manganite compounds of the general formula $La_{1-x}A_xMnO_3$ where A is Sr, Ca, Ba, or Mn and $x \sim 0.3$ (Refs. 14–20 and the present work). The $x \sim 0.3$ composition corresponds to the highest conductivity and is the most distant from phase boundaries;[50] in other words, phase separation effects should be the least significant here. This composition has also the highest spin-wave stiffness,[5,21] which indicates an increased length of the exchange interaction. The very fact that so far there is no indication of standing spin-wave resonances in manganite compounds with $x \neq 0.3$ (we also did not find any spin-wave resonances in $La_{0.8}Sr_{0.2}MnO_3$ films) may serve as indirect evidence of strong spin-wave scattering there.

VI. CONCLUSIONS

We measured the temperature dependence of the spin-wave stiffness in thin $La_{0.7}Sr_{0.3}MnO_3$ films as determined from the standing spin-wave resonances at microwave frequencies. The nonresonant microwave absorption in the same films is reported in the following paper.[51] At ambient temperature, the spin-wave stiffness of thin films and of single crystals is the same, while at low temperatures the spin-wave stiffness of thin films is enhanced with respect to that of a single crystal.

The spin-wave linewidth in our films is limited by the scattering at film interfaces. The very fact that we are able to observe spin-wave resonance in $La_{0.7}Sr_{0.3}MnO_3$ up to eighth order implies a high degree of coherence and very low bulk spin-wave scattering. This is important for spintronics and means that $La_{0.7}Sr_{0.3}MnO_3$ can be used as a spin-conserving component.

ACKNOWLEDGMENTS

We are grateful to Denis Golosov for illuminating discussions, to Xiangzhen Xu for help with the handling of the samples, and to Oscar Arnache who initiated these experiments.

*On leave from: The Racah Institute of Physics, The Hebrew University of Jerusalem, 91904 Jerusalem, Israel.
[1] C. Kittel, Phys. Rev. **110**, 1295 (1958).
[2] J. W. Lynn, R. W. Erwin, J. A. Borchers, Q. Huang, A. A. Santoro, J. L. Peng, and Z. Y. Li, Phys. Rev. Lett. **76**, 4046 (1996).
[3] M. C. Martin, G. Shirane, Y. Endoh, K. Hirota, Y. Moritomo, and Y. Tokura, Phys. Rev. B **53**, 14285 (1996).
[4] L. Vasiliu-Doloc, J. W. Lynn, Y. M. Mukovskii, A. A. Arsenov, and D. A. Shulyatev, J. Appl. Phys. **83**, 7342 (1998).
[5] A. H. Moudden, L. Vasiliu-Doloc, L. Pinsard, and A. Revcolevschi, Physica B **241**, 276 (1998).
[6] L. Vasiliu-Doloc, J. W. Lynn, A. H. Moudden, A. M. de Leon-Guevara, and A. Revcolevschi, Phys. Rev. B **58**, 14913 (1998).
[7] J. Zhang, F. Ye, Hao Sha, P. Dai, J. A. Fernandez-Baca, and E. W. Plummer, J. Phys.: Condens. Matter **19**, 315204 (2007).
[8] M. B. Salamon and M. Jaime, Rev. Mod. Phys. **73**, 583 (2001).
[9] C. E. Patton, Phys. Rep. **103**, 251 (1984).
[10] F. L. A. Machado, M. A. Lucena, A. E. P. de Araujo, A. Azevedo, F. M. de Aguiar, S. M. Rezende, and A. K. Nigam, Physica B **320**, 119 (2002).
[11] D. Talbayev, H. Zhao, G. Lupke, J. Chen, and Qi Li, Appl. Phys. Lett. **86**, 182501 (2005).
[12] M. Farle, Rep. Prog. Phys. **61**, 755 (1998).
[13] V. P. Denysenkov and A. M. Grishin, Rev. Sci. Instrum. **74**, 3400 (2003).
[14] S. E. Lofland, S. M. Bhagat, C. Kwon, M. C. Robson, R. P. Sharma, R. Ramesh, and T. Venkatesan, Phys. Lett. A **209**, 246 (1995).
[15] V. Dyakonov, A. Prohorov, V. Shapovalov, V. Krivoruchko, V. Pashchenko, E. Zubov, V. Mihailov, P. Aleshkevych, M. Berkowski, S. Piechota, and H. Szymczak, J. Phys.: Condens. Matter **13**, 4049 (2001).
[16] V. Dyakonov, A. Prohorov, V. Shapovalov, S. Khartsev, V. Krivoruchko, V. Mihailov, V. Pashchenko, E. Zubov, P. Aleshkevych, K. Dyakonov, S. Piechota, and H. Szymczak, Phys. Lett. A **268**, 202 (2000).
[17] P. Aleshkevych, M. Baran, V. Dyakonov, R. Szymczak, H. Szymczak, K. Baberschke, J. Lindner, and K. Lenz, Phys. Status Solidi A **203**, 1586 (2006).
[18] J. Yin, Y. X. Sui, J. H. Du, Y. X. Zhang, X. Y. Liu, and Z. G. Liu, Phys. Status Solidi A **174**, 499 (1999).
[19] A. I. Shames, E. Rozenberg, G. Gorodetsky, and M. Ziese, *Nanostructured Magnetic Materials and their Appllications* (Kluwer Academic, Dordrecht, 2004), pp. 205–212.
[20] D. L. Lyfar, S. M. Ryabchenko, V. N. Krivoruchko, S. I. Khartsev, and A. M. Grishin, Phys. Rev. B **69**, 100409(R) (2004).
[21] P. Aleshkevych, M. Baran, and H. Szymczak, Acta Phys. Pol. A **106**, 593 (2004).
[22] A. G. Gurevich and G. A. Melkov, *Magnetization Oscillations and Waves* (CRC Press, Boca Raton, 1996), p. 19.
[23] M. Golosovsky, M. Abu-Teir, D. Davidov, O. Arnache, P. Monod, N. Bontemps, and R. C. Budhani, J. Appl. Phys. **98**, 084902 (2005).
[24] K. Senapati and R. C. Budhani, Phys. Rev. B **71**, 224507 (2005).
[25] T. G. Phillips, Proc. R. Soc. London, Ser. A **292**, 224 (1966).
[26] Y. Suzuki, H. Y. Hwang, S. W. Cheong, and R. B. van Dover, Appl. Phys. Lett. **71**, 140 (1997).
[27] M. Ziese, H. C. Semmelhack, and P. Busch, J. Magn. Magn. Mater. **246**, 327 (2002).
[28] S. E. Lofland, S. M. Bhagat, C. Kwon, S. D. Tyagi, Y. M. Mukovskii, S. G. Karabashev, and A. M. Balbashov, J. Appl. Phys. **81**, 5737 (1997).
[29] L. Ranno, A. Llobet, R. Tiron, and E. Favre-Nicolin, Appl. Surf. Sci. **188**, 170 (2002).
[30] B. Wiedenhorst, C. Hofener, Yafeng Lu, J. Klein, L. Alff, R. Gross, B. H. Freitag, and W. Mader, Appl. Phys. Lett. **74**, 3636 (1999).
[31] A. A. Sidorenko, G. Allodi, R. De Renzi, G. Balestrino, and M. Angeloni, Phys. Rev. B **73**, 054406 (2006).
[32] N. Rosov, J. W. Lynn, J. Kastner, E. F. Wassermann, T. Chattopadhyay, and H. Bach, J. Appl. Phys. **75**, 6072 (1994).
[33] V. N. Smolyaninova, J. J. Hamilton, R. L. Greene, Y. M. Mukovskii, S. G. Karabashev, and A. M. Balbashov, Phys. Rev. B **55**, 5640 (1997).
[34] S. Budak, M. Ozdemir, and B. Aktas, Physica B **339**, 45 (2003).
[35] T. Rossing and T. G. Phillips, J. Appl. Phys. **39**, 1375 (1968).
[36] U. Kobler, A. Hoser, and W. Schafer, Physica B **364**, 55 (2005).
[37] Our measurements were performed with the thermocouple mounted at some distance from the sample. Since thermalization is slow, to restrict the duration of the experiment to several hours, in some experimental runs we slowly heated the sample from low temperature and measured the spectra in a continuous way without waiting for thermalization. In such experiments we determine only D and H_a.
[38] P. Lubitz, S. M. Bhagat, G. C. Bailey, and C. Vittoria, Phys. Rev. B **11**, 3585 (1975).
[39] G. Suran and R. J. Gambino, J. Appl. Phys. **50**, 7671 (1979).
[40] F. Schreiber and Z. Frait, Phys. Rev. B **54**, 6473 (1996).
[41] C. G. Bailey and C. Vittoria, Phys. Rev. Lett. **28**, 100 (1972).
[42] T. G. Phillips and H. M. Rosenberg, Rep. Prog. Phys. **29**, 285 (1966).
[43] J. C. S. Levy, Phys. Rev. B **25**, 2893 (1982).
[44] D. I. Golosov, Phys. Rev. Lett. **84**, 3974 (2000).
[45] Y. Motome and N. Furukawa, Phys. Rev. B **71**, 014446 (2005).
[46] U. Hoeppe and H. Benner, Phys. Rev. B **71**, 144403 (2005).
[47] D. G. Scotter, J. Phys. D **5**, L93 (1972).
[48] A. Azevedo, A. B. Oliveira, F. M. de Aguiar, and S. M. Rezende, Phys. Rev. B **62**, 5331 (2000).
[49] M. P. de Jong, I. Bergenti, V. A. Dediu, M. Fahlman, M. Marsi, and C. Taliani, Phys. Rev. B **71**, 014434 (2005).
[50] M. Imada, A. Fujimori, and Y. Tokura, Rev. Mod. Phys. **70**, 1039 (1998).
[51] M. Golososky, P. Monod, P. K. Muduli, R. C. Budhani, L. Mechin, and P. Perna, following paper, Phys. Rev. B **76**, 184414 (2007).